Effects of a Moving Mass on the Dynamic Behavior of Cantilever Beams with Double Cracks

In-Soo Son[1,#], Jeong -Rae Cho[2] and Han-Ik Yoon[1]

1 School of Mechanical Engineering, Dong-eui University, 995 Eomgwangno, Busanjin-gu, Busan, South Korea, 614-714
2 Department of Car-Electronics, Korea Polytechnic VI Collage Dalseong Campus, 717-3, Nongong-eub, Dalseong-gun, Daegu, South Korea, 711-852
Corresponding Author / E-mail: isson92@deu.ac.kr, TEL: +82-51-890-2239, FAX: +82-51-890-2232

KEYWORDS: Dynamic behavior, Cantilever beam, Double-crack, Moving mass, Tip mass

The effects of a double crack and tip masses on the dynamic behavior of cantilever beams with a moving mass are studied using numerical methods. The cantilever beams are modeled by applying Euler–Bernoulli beam theory. The cracked sections are represented by a local flexibility matrix connecting three undamaged beam segments. The influences of the crack, moving mass, and tip mass, and the coupling of these factors on the vibration mode and the frequencies of the double-cracked cantilever beams are determined analytically. The methodology provides a basis for analyzing the dynamic behavior of a beam with an arbitrary number of cracks and a moving mass.

Manuscript received: August 22, 2007 / Accepted: April 7, 2008

1. Introduction

The effect of cracks on the dynamic behavior of structural elements has been the subject of several investigations. When a structure is subjected to damage, its dynamic response will vary due to changes in its mechanical characteristics. The effect of a moving mass on structures and machines is an important problem, both in the field of transportation and in the design of machining processes. In practice, two or more cracks may exist in a structure, resulting in complicated vibration phenomena. Therefore, studying the influences of these factors on the dynamic characteristics of a structure is important.

Many studies on the dynamic behavior of a beam structure under a moving load and moving mass have been reported[1–3]. Recently, Mahmoud and Zaid[4] used an equivalent static load approach to determine the stress intensity factors for a single-edge crack in a beam subjected to a moving load. Chondros and Dimarogonas[5,6] studied the effect of the crack depth on the dynamic behavior of a cantilevered beam and showed that the natural frequency of the beam decreased with increasing crack depths. They also used an energy method and the continuous cracked beam theory to analyze the transverse vibrations of cracked beams. Narkis[7] demonstrated that if the crack on rod is very small, the only information required for accurate crack localization is the ratio between the variations of the first two natural frequencies caused by the crack. Lin[8] used direct and inverse methods to analyze the free vibrations of a simply supported beam with a crack. These methods were based on Timoshenko beam theory and presented the crack as a massless rotational spring. Liu *et al.*[9] examined the suitability of using coupled responses to detect damage in thin-walled tubular structures. Here, coupled response referred to the stability of a structural member with a circumferential crack when describing composite vibration modes (axial and bending) excited by purely lateral forces. Recently, Yoon *et al.*[10] investigated the effects of an open crack and a moving mass on the dynamic behavior of the crack and the moving mass and its velocity. They also examined how the coupling of these factors affected the dynamic behavior of a Timoshenko beam.

Most crack detection studies have concentrated on analyzing the effect of a single crack on the dynamics of a simple structure, such as a shaft and a beam. The dynamic behavior of a double-cracked beam and a rotor with two cracks were investigated by Ruotolo *et al.*[11] and Shekar[12], respectively. Ostachowicz and Krawczuk[13] investigated the influence of the position and depth of two open cracks on the fundamental frequency of the natural flexural vibrations of a cantilever beam. They introduced two different functions according to the symmetry of the crack to model the effect of the local stress in the crack. Shen and Pierre[14] considered the same problem for symmetric cracks. An equation for the bending motion of an Euler–Bernoulli beam containing pairs of symmetrical open cracks was derived by Christides and Barr[15]. The cracks were normal to the beam's neutral axis and symmetrical about the plane of bending. Douka *et al.*[16] proposed a method for determining the location and depth of the cracks in double-cracked beams.

In this report, the effects of each crack on the dynamic behavior of double-cracked cantilever beams with a moving mass and tip masses are investigated. The influence of each crack, the tip mass, and the velocity of the moving mass are examined in detail. The cantilever beams are modeled using Euler–Bernoulli beam theory.

2. Mathematical Model

A double-cracked cantilever beam system with a moving mass and a tip mass is shown in Fig. 1, where M_m is the moving mass, V is the velocity of the moving mass, L is the total length of the beam, and m_p

is the tip mass. In Fig. 1(b), x_{c1} and x_{c2} are the positions of each crack from the left-hand clamped end, and K_1 and K_2 are the bending spring constant at crack positions x_{c1} and x_{c2}, respectively.

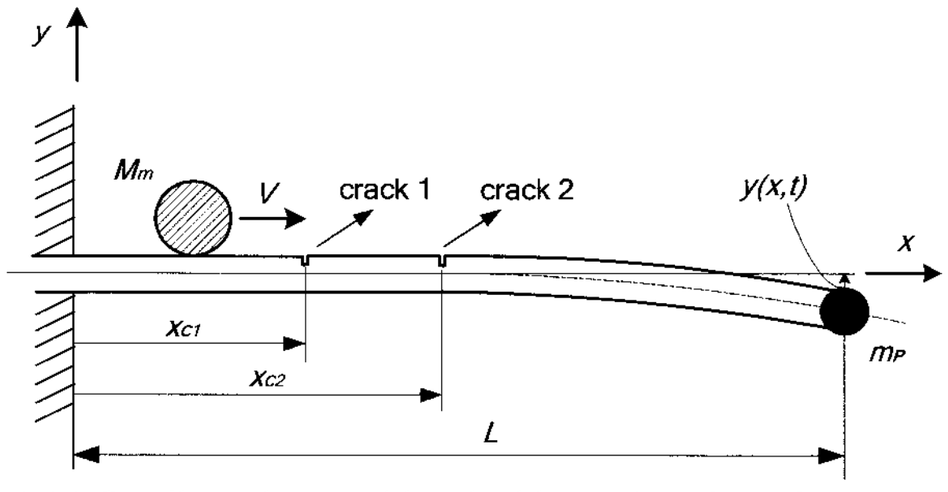

Fig. 1 (a) Cantilever beam with a double crack and moving mass

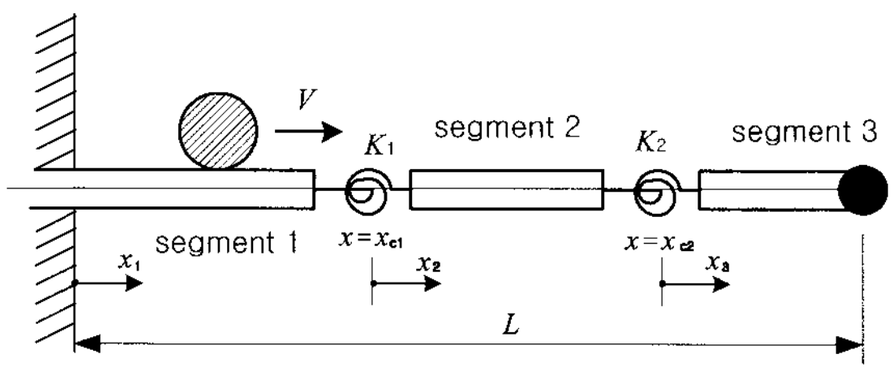

Fig. 1 (b) Model of the double-cracked cantilever beam

Figure 2(a) and (b) show cross sections of the cracked portion of circular and rectangular beams. In Fig. 2(a), a_c and $2b$ are the crack depth and width, respectively. In Fig. 2(b), b and h are the rectangular cross-sectional dimensions. Three equations of motion can derived for the three parts of the beam separated by the cracked sections.

2.1 Crack model

Consider the bending vibrations of a uniform Euler–Bernoulli beam in the x–y plane, which is assumed to be a plane of symmetry for any cross section. Assume also that the crack is always open. The additional strain energy due to the crack can be considered in the form of a flexibility coefficient expressed in terms of the stress intensity factor, which can be derived using Castigliano's theorem in the linear elastic range. Therefore the local flexibility in the presence of a crack with a width of $2b$ is defined by[17]

$$C_{ij} = \frac{\partial u_{ij}}{\partial P_j} = \frac{\partial^2}{\partial P_i \partial P_j}\left(\int_{-b}^{b} \int_{0}^{a_c} J(\alpha)\, d\alpha dz \right), \tag{1}$$

where P_i is the load in the same direction as the displacement and $J(\alpha)$ is the strain energy density function

$$J(\alpha) = \frac{1}{E^*}\left(K_{IP} + K_{IM}\right)^2 \tag{2}$$

and $E^* = E/(1 - \nu_p^2)$ for the plane strain and ν_p is Poisson's ratio. Since the cracks are assumed to be always open during vibrations, the contribution of the mode (II) stress intensity factor will be neglected.[17] The stress intensity factors for fracture mode (I) due to force P and moment M, K_{IP} and K_{IM}, are given by

i) Case I: beam with a circular cross section [Fig. 2(a)]

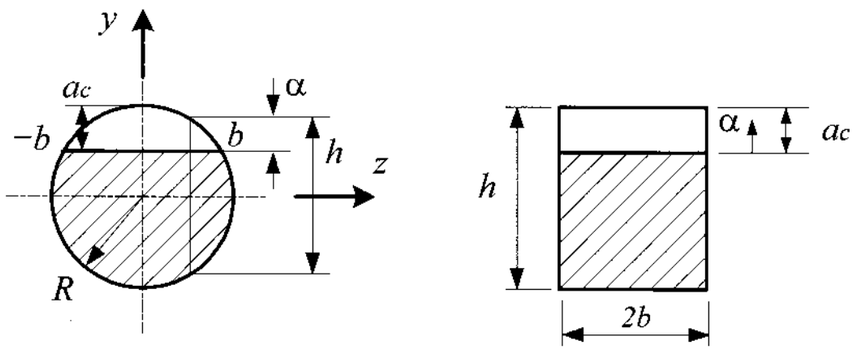

(a) Circular cross section (b) Rectangular cross section

Fig. 2 Geometry of the cracked section of beams

$$K_{IP} = \frac{P}{\pi R^2}\sqrt{R^2 - z^2}\sqrt{\pi\alpha}\; F_I\left(\frac{\alpha}{h}\right),$$
$$K_{IM} = \frac{4M}{\pi R^4}\sqrt{R^2 - z^2}\sqrt{\pi\alpha}\; F_{II}\left(\frac{\alpha}{h}\right) \tag{3}$$

ii) Case II: beam with a rectangular cross section [Fig. 2 (b)]

$$K_{IP} = \frac{P}{bh}\sqrt{\pi\alpha}\; F_I\left(\frac{\alpha}{h}\right),$$
$$K_{IM} = \frac{6M}{bh^2}\sqrt{\pi\alpha}\; F_{II}\left(\frac{\alpha}{h}\right) \tag{4}$$

where

$$F_I\left(\frac{\alpha}{h}\right) = \sqrt{\frac{\tan(\varsigma)}{\varsigma}}\,\frac{\left[0.752 + 2.02\left(\frac{\alpha}{h}\right) + 0.37\left(1 - \sin(\varsigma)\right)^3\right]}{\cos(\varsigma)},$$
$$F_{II}\left(\frac{\alpha}{h}\right) = \sqrt{\frac{\tan(\varsigma)}{\varsigma}}\,\frac{\left[0.923 + 0.199\left(1 - \sin(\varsigma)\right)^4\right]}{\cos(\varsigma)} \tag{5}$$

and $\varsigma = \pi\alpha/(2h)$. The flexible matrix due to the crack can be obtained by substituting Eqs. (3)–(5) into Eq. (1).

2.2 Energy of the beam and moving mass

In Fig. 1, the energy of the cracked cantilever beam with a tip mass can be written as[18]

$$T_p = \frac{1}{2}m\left[\int_0^{x_{c1}}\left\{\frac{\partial y_1(x,t)}{\partial t}\right\}^2 dx + \int_{x_{c1}}^{x_{c2}}\left\{\frac{\partial y_2(x,t)}{\partial t}\right\}^2 dx + \int_{x_{c2}}^{L}\left\{\frac{\partial y_3(x,t)}{\partial t}\right\}^2 dx\right] + \frac{1}{2}m_p\left\{\frac{\partial y_3(L,t)}{\partial t}\right\}^2, \tag{6}$$

$$V_p = \frac{1}{2}EI\left[\int_0^{x_{c1}}\left\{\frac{\partial^2 y_1(x,t)}{\partial x^2}\right\}^2 dx + \int_{x_{c1}}^{x_{c2}}\left\{\frac{\partial^2 y_2(x,t)}{\partial x^2}\right\}^2 dx + \int_{x_{c2}}^{L}\left\{\frac{\partial^2 y_3(x,t)}{\partial x^2}\right\}^2 dx\right] + \frac{K_1}{2}\left(\frac{y_2(x_{c1},t)}{\partial x} - \frac{y_1(x_{c1},t)}{\partial x}\right)^2 + \frac{K_2}{2}\left(\frac{y_3(x_{c2},t)}{\partial x} - \frac{y_2(x_{c2},t)}{\partial x}\right)^2, \tag{7}$$

where m and EI are the mass per unit length of pipe and the bending stiffness, respectively. Here, y_1, y_2, and y_3 are

$$y_k(x,t) = \sum_{i=1}^{n}\sum_{k=1}^{3}\phi_{ki}(x)q_i(t), \tag{8}$$

where $q_i(t)$ are generalized time-dependent coordinates, n is the total number of the generalized coordinates, $\phi_i(x)$ are the spatial mode functions of the cantilever beam, and k(= 1,2,3) are the numbers of segments.

The kinetic energy of a moving mass can be expressed as follows[18]:

$$T_M = \frac{M_m}{2}\sum_{k=1}^{3}\left\{V^2\left(\frac{\partial y_k(x_m,t)}{\partial x}\right)^2 + 2V\left(\frac{\partial y_k(x_m,t)}{\partial x}\right)\left(\frac{\partial y_k(x_m,t)}{\partial t}\right) + \left(\frac{\partial y_k(x_m,t)}{\partial t}\right)^2 + V^2\right\}. \tag{9}$$

Since the horizontal velocity of the moving mass is V, the horizontal displacement of the moving mass x_m is

$$x_m = f_m(t) = \int_0^t V\, dt \qquad (\,0 \le x_m \le L\,). \tag{10}$$

2.3 Equations of motion

2.3.1 Dimensionless equations of motion

The equations of motion of the system can be obtained by substituting the above energy functions into Hamilton's principle:[19]

$$\int_{t_1}^{t_2}\left(\delta T_p + \delta T_M - \delta V_p\right) dt = 0\,. \tag{11}$$

For simplicity, the following dimensionless quantities are introduced:

$$\xi = \frac{x}{L}, \qquad \tau = \frac{t}{L^2}\sqrt{\frac{EI}{m}}, \qquad C_D = \frac{a_c}{h}, \qquad \xi_c = \frac{x_c}{L},$$
$$\mu = \frac{M_m}{mL}, \qquad v = V\sqrt{\frac{M_m L}{EI}}, \qquad M_p = \frac{m_p}{mL}, \tag{12}$$
$$\xi_m = \frac{x_m}{L} = VL\sqrt{\frac{m}{EI}}\ \tau, \qquad k_1 = \frac{K_1 L}{EI}, \qquad k_2 = \frac{K_2 L}{EI}.$$

The dimensionless quantity η_k is given by

$$\eta_k = \frac{y_k}{L} = \sum_{i=1}^{n}\sum_{k=1}^{3}\phi_{ki}(\xi)d_i(\tau)\,, \tag{13}$$

where $\phi_{ki}(\xi)$ can be described as follows:

I) segment 1 ($0 \le \xi \le \xi_{c1}$)

$$\phi_{1i}(\xi) = A_1\cos(\lambda_i\xi) + A_2\sin(\lambda_i\xi) + A_3\cosh(\lambda_i\xi) + A_4\sinh(\lambda_i\xi) \tag{14a}$$

II) segment 2 ($\xi_{c1} \le \xi \le \xi_{c2}$)

$$\phi_{2i}(\xi) = A_5\cos(\lambda_i\xi) + A_6\sin(\lambda_i\xi) + A_7\cosh(\lambda_i\xi) + A_8\sinh(\lambda_i\xi) \tag{14b}$$

III) segment 3 ($\xi_{c2} \le \xi \le 1$)

$$\phi_{3i}(\xi) = A_9\cos(\lambda_i\xi) + A_{10}\sin(\lambda_i\xi) + A_{11}\cosh(\lambda_i\xi) + A_{12}\sinh(\lambda_i\xi)\,. \tag{14c}$$

Here, λ_i is the frequency parameter, which can be calculated using the frequency equation of a cantilever beam[20]. In Eq. (14), the constants $A_1, A_2, \ldots, A_{12}$ can be found from the boundary conditions of the beam and the continuity conditions for the transverse deflection, bending moment, shear force, and slope at the each crack. Therefore, the dimensionless equations of motion can be written in matrix form as follows:

$$\mathbf{M}\ddot{\mathbf{d}} + \mathbf{C}\dot{\mathbf{d}} + \mathbf{K}\mathbf{d} = \mathbf{0}\,, \tag{15}$$

where $(\cdot)$ denotes $\partial/\partial\tau$. The matrices of Eq. (15) can be written as

$$\mathbf{M} = \sum_{i=1}^{n}\left[\left(\mathbf{M}\right)_{ij} + \mu\left(\mathbf{M_m}\right)_{ij} + M_p\left(\mathbf{M_p}\right)_{ij}\right] \tag{16}$$

$$\mathbf{C} = \sum_{i=1}^{n}\left[2v\sqrt{\mu}\left(\mathbf{M_m}\right)_{ij}\right] \tag{17}$$

$$\mathbf{K} = \sum_{i=1}^{n}\left[\left(\mathbf{K}\right)_{ij} + v^2\left(\mathbf{K_m}\right)_{ij}\right]. \tag{18}$$

These are defined as

$$\left(\mathbf{M}\right)_{ij} = \int_0^{\xi_{c1}}\phi_{i1}(\xi)\phi_{j1}(\xi)\,d\xi + \int_{\xi_{c1}}^{\xi_{c2}}\phi_{i2}(\xi)\phi_{j2}(\xi)\,d\xi + \int_{\xi_{c2}}^{1}\phi_{i3}(\xi)\phi_{j3}(\xi)\,d\xi \tag{19}$$

$$\left(\mathbf{M_m}\right)_{ij} = \sum_{k=1}^{3}\left[\phi_{ki}(\xi_m)\phi_{kj}(\xi_m)\right] \tag{20}$$

$$\left(\mathbf{M_p}\right)_{ij} = \phi_{3i}(1)\phi_{3j}(1) \tag{21}$$

$$\left(\mathbf{K}\right)_{ij} = \int_0^{\xi_{c1}}\phi_{1i}(\xi)\,\phi_{1j}''''(\xi)\,d\xi + \int_{\xi_{c1}}^{\xi_{c2}}\phi_{2i}(\xi)\,\phi_{2j}''''(\xi)\,d\xi + \int_{\xi_{c2}}^{1}\phi_{3i}(\xi)\,\phi_{3j}''''(\xi)\,d\xi \tag{22}$$

$$\left(\mathbf{K_m}\right)_{ij} = \sum_{k=1}^{3}\left[\phi_{ki}(\xi_m)\phi_{kj}''(\xi_m)\right] \tag{23}$$

where $(')$ denotes $\partial/\partial\xi$.

2.3.2 Modal formulation

We assume that the displacement field varies with time according to an exponential law,

$$\mathbf{d}(\tau) = \mathbf{X}e^{\omega\tau}\,, \tag{24}$$

where ω is the complex eigenvalue and $\mathbf{X}$ is the corresponding mode shape. Combining Eqs. (15) and (24),

$$\omega\boldsymbol{\eta} = \mathbf{A}\boldsymbol{\eta} \tag{25}$$

and

$$\boldsymbol{\eta} = \begin{bmatrix}\mathbf{X} & \dot{\mathbf{X}}\end{bmatrix}^{\mathrm{T}}, \quad \mathbf{A} = \begin{bmatrix}\mathbf{0} & \mathbf{I} \\ -\mathbf{M}^{-1}\mathbf{K} & -\mathbf{M}^{-1}\mathbf{C}\end{bmatrix}, \tag{26}$$

where $\mathbf{I}$ represents a unit matrix. The natural frequencies of the system can be obtained from the eigenvalues in Eqs. (24)–(26).

3. Numerical Results and Discussion

The dynamic behavior of cracked cantilever beams is influenced by the moving mass, crack depth, tip mass, and position of the crack. These were computed using a fourth-order Runge–Kutta method. We studied the dynamic behavior of double-cracked cantilever beams for the first mode of vibration. The properties of the cracked cantilever beams are listed in Table 1. The velocity of the moving mass was held constant at 1 m/s.

Table 1 Specifications of the cantilever beams

	Case I: circular cross-sectional beam	Case II: rectangular cross-sectional beam
Cross-sectional area	$\pi R^2 = 0.002$ m^2	$B \times h = 0.002$ m^2
Young's modulus	208 GPa	208 GPa
Material density	7850 kg/m^3	7850 kg/m^3
Length of beam	1 m	1 m
Moment of inertia	3.07E-7 m^4	4.17E-7 m^4

Figure 3 shows the natural frequencies of single-cracked cantilever beams without a tip mass for a moving mass with $\mu = 0.5$ and $\xi_c = 0.3$. The horizontal axis gives the position of moving mass while the vertical axis gives the frequency of the cracked cantilever beam. Case I is a beam with a circular cross section while Case II is a beam with a rectangular cross section. When the ratio of the crack depth was constant, the frequency of the cantilever beam decreased as the moving mass moved to the free end of the cantilever beam. The small difference between the natural frequencies of Cases (I) and (II) was due to the different moments of inertia (see Table 1).

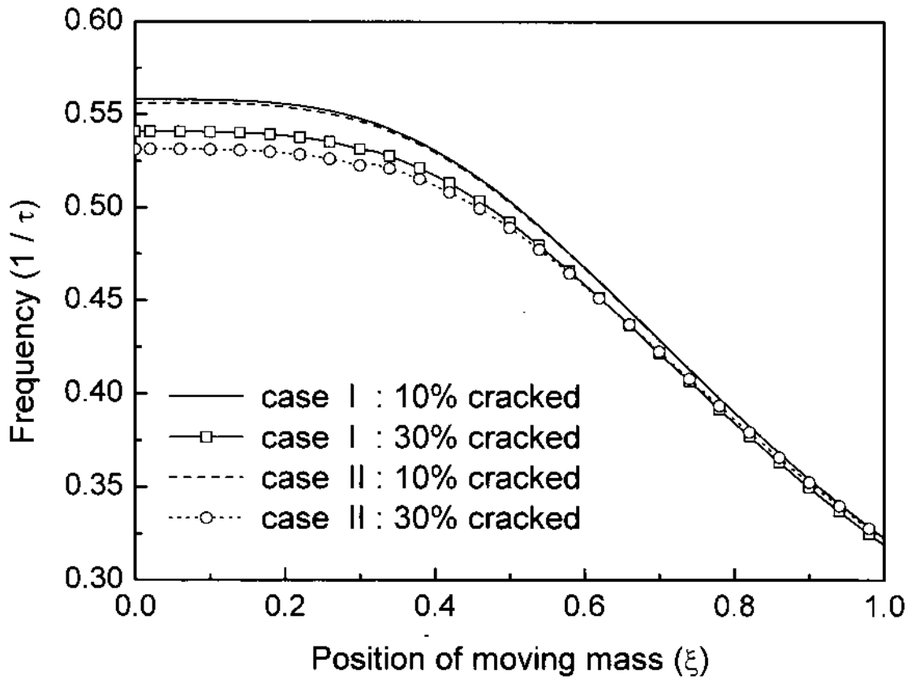

Fig. 3 Natural frequencies of cracked beams with a circular cross-sections (Case I) and a rectangular cross sections (Case II), $\mu = 0.5$ and $\xi_c = 0.3$

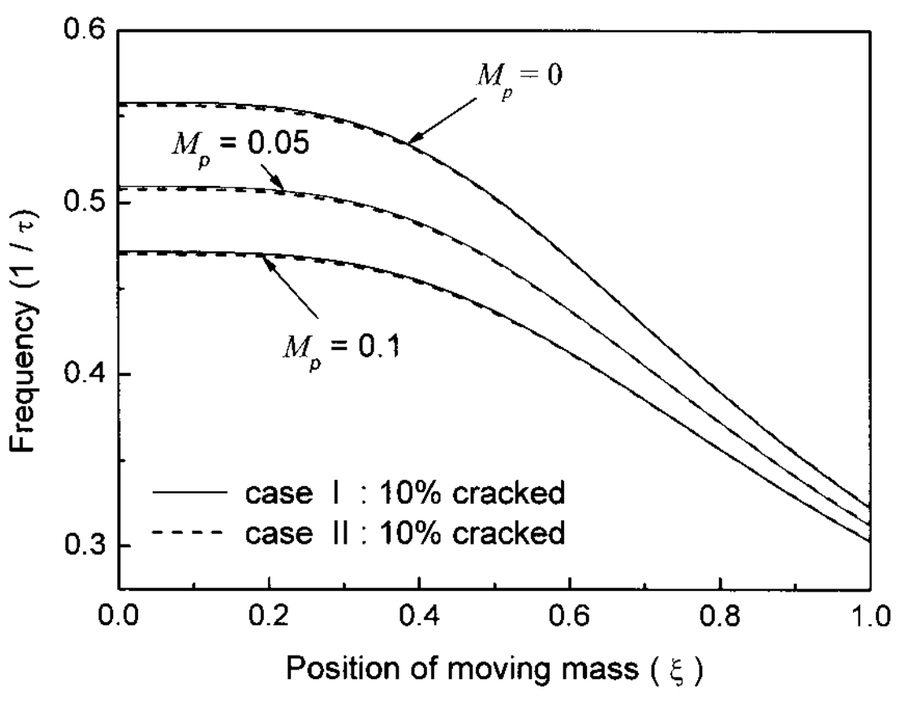

(a) Single-cracked beams ($\xi_c = 0.3$)

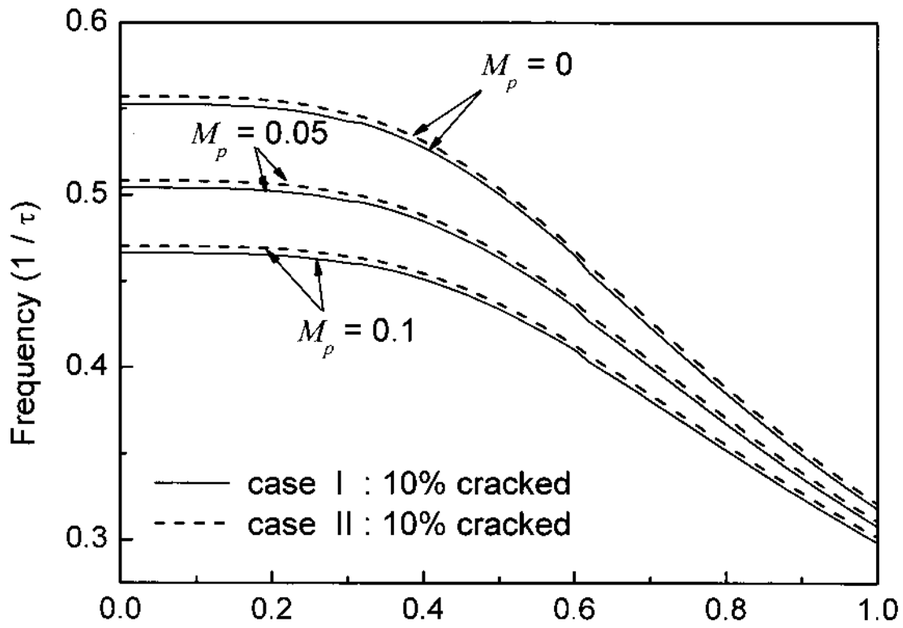

(b) Double-cracked beams ($\xi_{c1} = 0.3$, $\xi_{c2} = 0.6$)

Fig. 4 Natural frequencies of cracked beams with different tip masses

Table 2 Natural frequency ratios (cracked/uncracked) of the present results and other studies for a single-cracked beam: Case II

	ξ_c	Crack depth (C_D)			
		0.2	0.25	0.4	0.6
Present results	0.2	0.99276	0.98803	0.96633	0.80523
	0.4	0.99707	0.99512	0.98530	0.91074
Ref. 21	0.2	0.9837	-	0.9614	0.8122
	0.4	0.9933		0.9709	0.9091
Ref. 14	0.2	-	0.9817	0.9520	0.8213

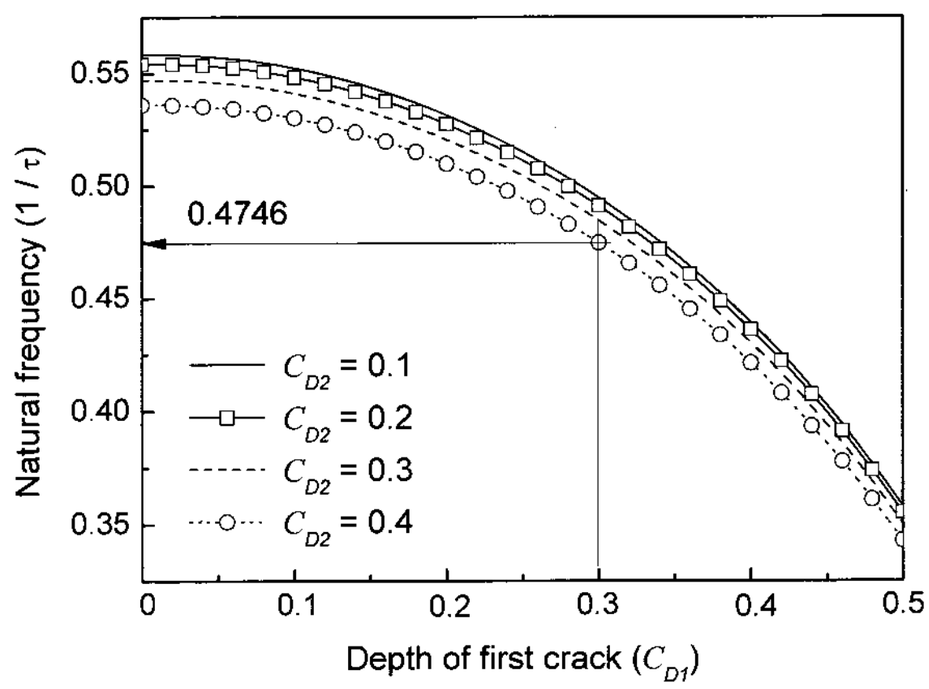

Fig. 5 Natural frequencies of double-cracked beams versus the depth of the first crack ($\xi_{c1} = 0.3$, $\xi_{c2} = 0.6$, $\mu = 0$)

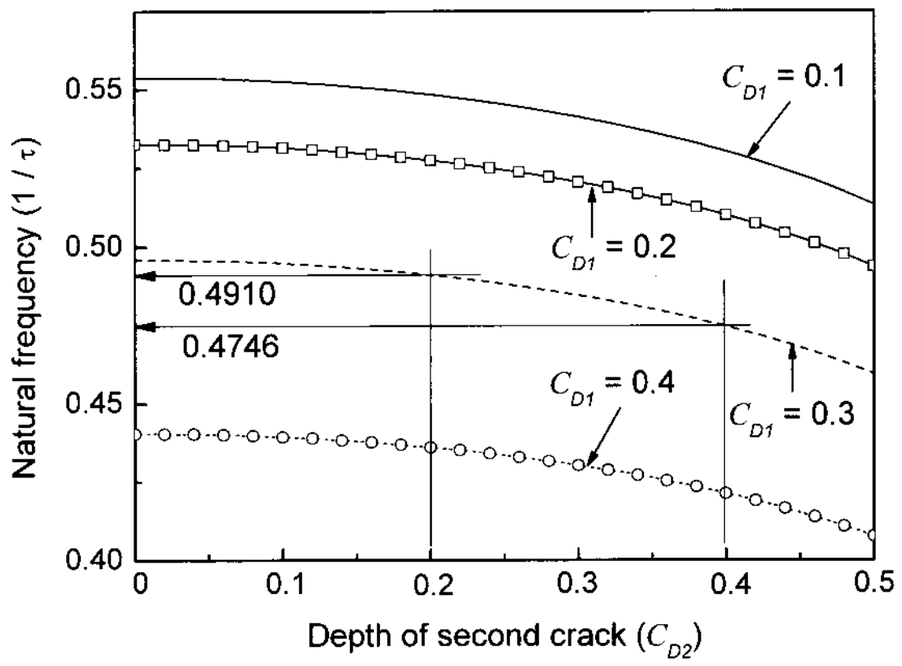

Fig. 6 Natural frequencies of double-cracked beams versus the depth of the second crack ($\xi_{c1} = 0.3$, $\xi_{c2} = 0.6$, $\mu = 0$)

Figure 4 shows the frequencies of cracked cantilever beams with different tip masses for a moving mass with $\mu = 0.5$. The results for single-cracked beams with $\xi_c = 0.3$ are plotted in Fig. 4(a), while the results for double-cracked beams for $\xi_{c1} = 0.3$ and $\xi_{c2} = 0.6$ are plotted in Fig. 4(b). The natural frequencies of the cracked cantilever beams were proportional to the tip mass. For Case I, the natural frequency of a single-cracked beam without a tip mass increased to 15.7% above the $M_p = 0.1$ curve, while that of a double-cracked beam without a tip mass increased to 15.1% above the $M_p = 0.1$ curve.

Table 2 compares the ratios of the natural frequencies of single-cracked cantilever beams without a moving mass obtained from the present results and from others studies in the literature. The dimensions of the beams with rectangular cross sections were $L = 0.2$ m, $h = 0.0078$ m, and $b = 0.025$ m.

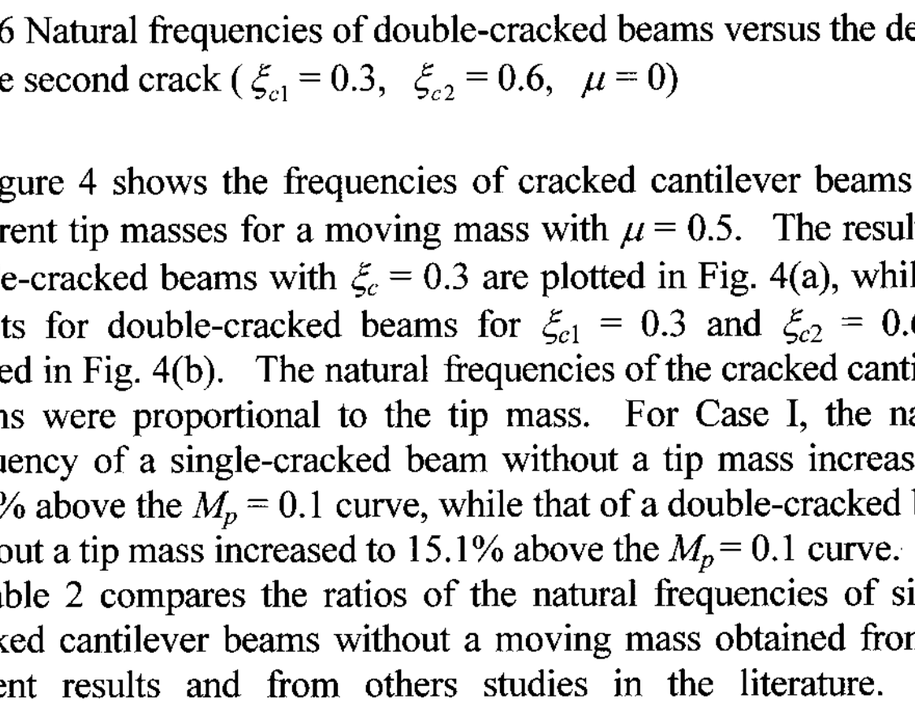

(a) Second crack depth: $C_{D2} = 0.2$

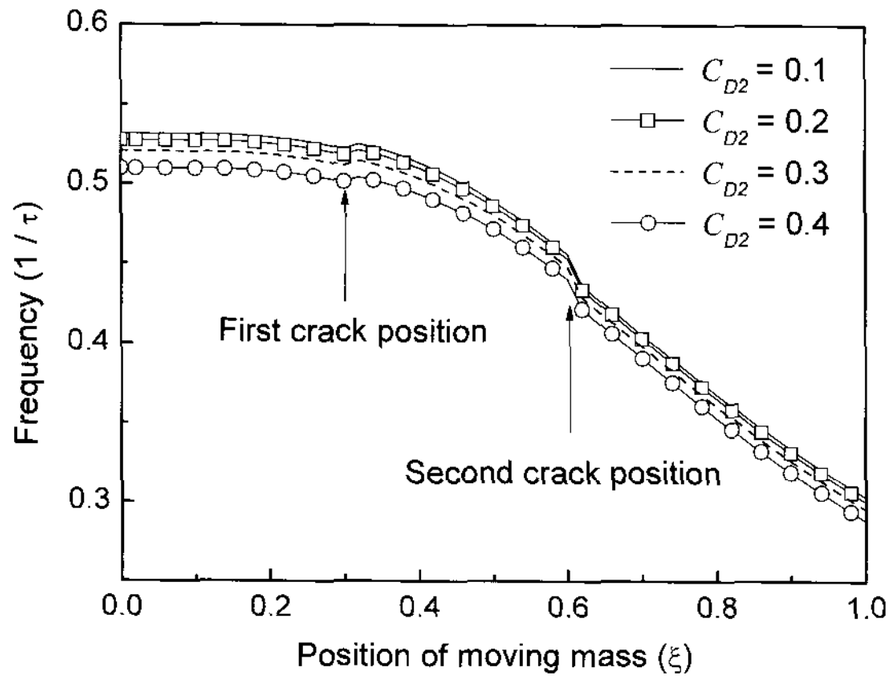

(b) First crack depth: $C_{D1} = 0.2$

Fig. 7 Variation in the natural frequencies of double-cracked beams due to the crack depth ($\xi_{c1} = 0.3$, $\xi_{c2} = 0.6$, $\mu = 0.5$)

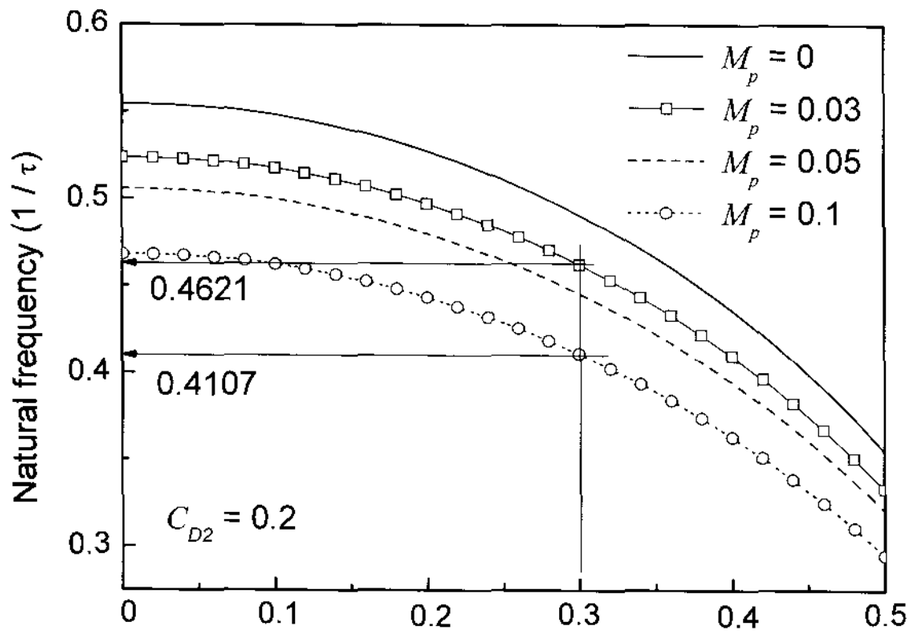

Fig. 8 Variation in the natural frequencies of double-cracked beams due to the tip mass ($\xi_{c1} = 0.3$, $\xi_{c2} = 0.6$, $\mu = 0$, $C_{D2} = 0.2$)

Figures 5 and 6 show the natural frequencies of double-cracked cantilever beams without a moving mass as functions of the crack depth. The double cracks were located at $\xi_{c1} = 0.3$ and $\xi_{c2} = 0.6$ from the clamped end of the beam. We could easily predict the natural frequencies of the beams, and the changes in the natural frequencies could be used to estimate the depth of the cracks. Conversely, changes in the depth of the cracks could be used to estimate the natural frequencies of the beams. In Fig. 6, we plotted the change in the natural frequency versus the depth of the second crack, C_{D2}, for four different values of the depth of the first crack, C_{D1}.

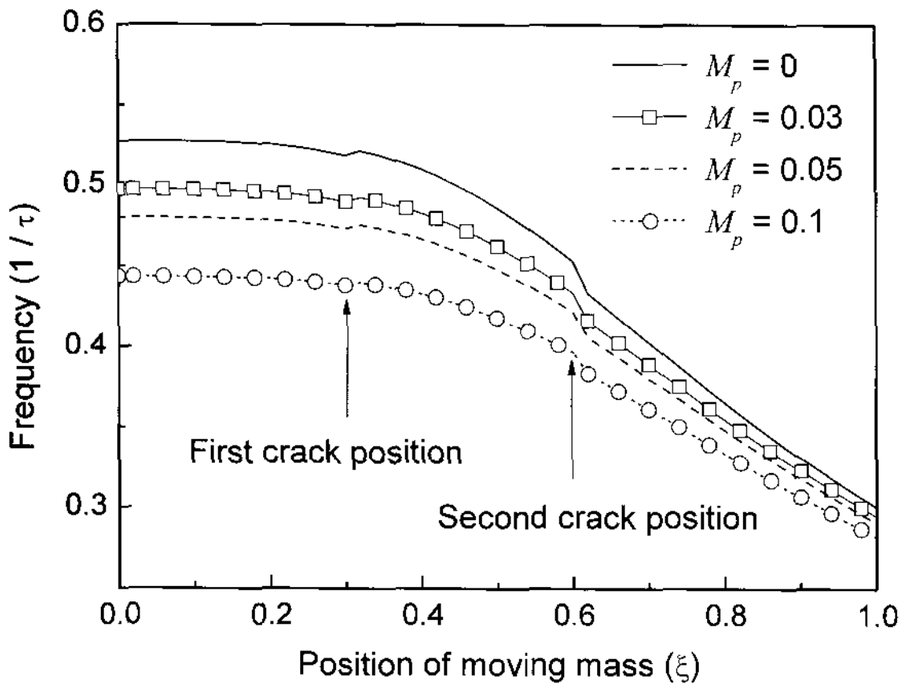

Fig. 9 Variation in the natural frequencies of double-cracked beams due to the tip mass ($\xi_{c1} = 0.3$, $\xi_{c2} = 0.6$, $\mu = 0.5$, $C_{D1} = 0.2$, $C_{D2} = 0.2$)

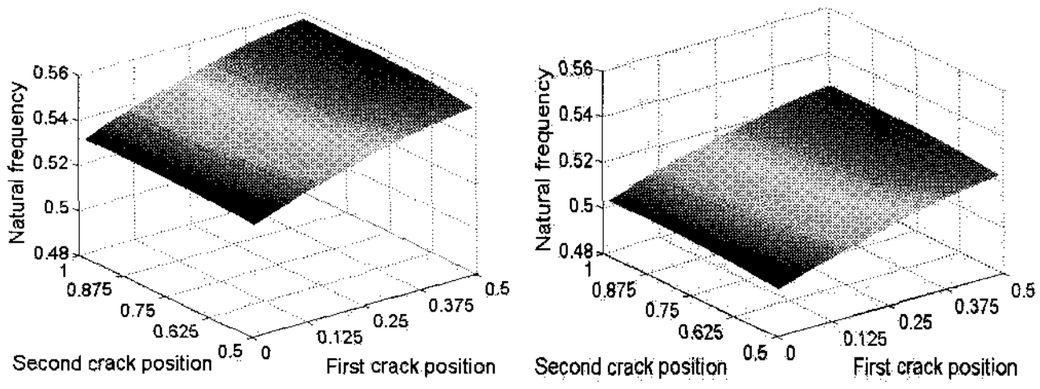

(a) $M_p = 0$ (b) $M_p = 0.03$

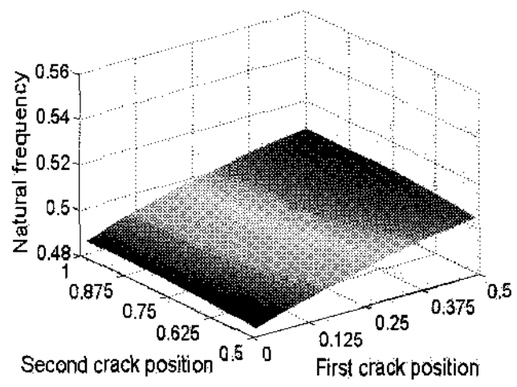

(c) $M_p = 0.05$

Fig. 10 Contours of the natural frequencies of double-cracked beams due to the tip mass and crack position ($C_{D1} = C_{D2} = 0.2$, $\mu = 0$)

A horizontal line could be drawn using the measured natural frequencies of the cracked beams. The intersection of this line with the C_{D1} curves represents the depth of the first crack, while the ordinate of the intersection point represents the depth of the second crack. In our example, we estimated that the natural frequency of the cracked beam was 0.4746 when the depths of the cracks were $C_{D1} = 0.3$ and $C_{D2} = 0.4$. When the depths of the cracks were $C_{D1} = 0.3$ and $C_{D2} = 0.2$, we estimated that the natural frequency of the cracked beam was 0.4910.

Table 3 Natural frequencies of double-cracked circular cross-sectional beams with different tip masses ($\xi_{c1} = 0.3$, $\xi_{c1} = 0.6$, $\mu = 0$)

M_p	C_{D1} = 0.2			C_{D2} = 0.2		
	C_{D2} = 0.1	C_{D2} = 0.2	C_{D2} = 0.3	C_{D1} = 0.1	C_{D1} = 0.2	C_{D1} = 0.3
0	0.5314	0.5274	0.5205	0.5483	0.5274	0.4910
0.03	0.5013	0.4974	0.4906	0.5177	0.4974	0.4622
0.05	0.4838	0.4799	0.4733	0.4999	0.4799	0.4456
0.10	0.4470	0.4433	0.4370	0.4624	0.4433	0.4108

Table 4 Natural frequencies of double-cracked rectangular cross-sectional beams with different tip masses ($\xi_{c1} = 0.3$, $\xi_{c1} = 0.6$, $\mu = 0$)

M_p	C_{D1} = 0.2			C_{D2} = 0.2		
	C_{D2} = 0.1	C_{D2} = 0.2	C_{D2} = 0.3	C_{D1} = 0.1	C_{D1} = 0.2	C_{D1} = 0.3
0	0.5509	0.5495	0.5470	0.5555	0.5495	0.5384
0.03	0.5200	0.5186	0.5162	0.5247	0.5186	0.5076
0.05	0.5021	0.5007	0.4983	0.5068	0.5007	0.4898
0.10	0.4643	0.4630	0.4606	0.4689	0.4630	0.4525

The natural frequencies of a double-cracked beam due to the depth of the crack are shown in Fig. 7. The positions of the cracks were $\xi_{c1} = 0.3$ and $\xi_{c2} = 0.6$, and the moving mass was located at 0.5. The frequencies of the cracked cantilever beam decreased as the depth of the cracks increased. A striking change was observed in the slope of the curves in the vicinity of the cracks. Therefore, we could determine the position of the cracks in the beam from the sharp changes in the slopes of the frequency curves.

Figure 8 shows the natural frequencies of double-cracked cantilever beams with tip masses. The positions of the cracks were $\xi_{c1} = 0.3$ and $\xi_{c2} = 0.6$. When the tip mass was 0.1, the depths of the

cracks were $C_{D1} = 0.3$ and $C_{D2} = 0.2$, leading to a cracked-beam natural frequency of 0.4107.

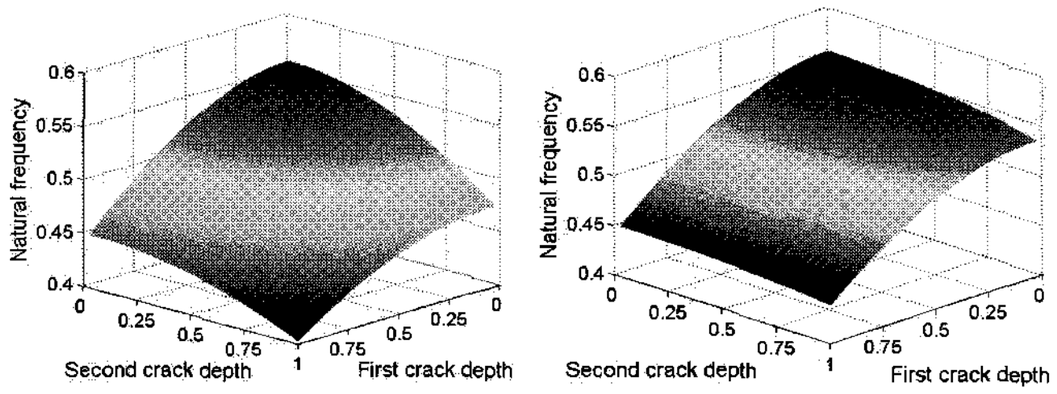

(a) $\xi_{c1} = 0.1, \xi_{c2} = 0.2, M_p = 0$ (b) $\xi_{c1} = 0.1, \xi_{c2} = 0.5, M_p = 0$

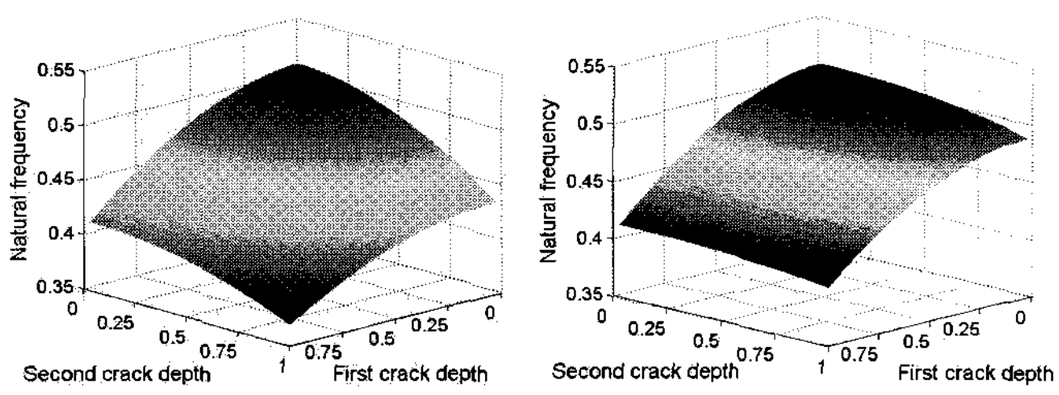

(c) $\xi_{c1} = 0.1, \xi_{c2} = 0.2, M_p = 0.05$ (d) $\xi_{c1} = 0.1, \xi_{c2} = 0.5, M_p = 0.05$

Fig. 11 Contours of the natural frequencies of double-cracked beams due to the tip mass and crack depth ($\mu = 0$)

Figure 9 shows the natural frequencies of double-cracked cantilever beams with different tip masses and a moving mass. When the moving mass was located at the left-hand clamped end of the cantilever beam, the frequencies of the cantilever beam were more sensitive to the effects of the tip mass.

Figures 10 and 11 show the natural frequencies of double-cracked cantilever beams due to the crack position, depths of the cracks, and tip mass. In Fig. 10, the position of the first crack moved from the left-hand clamped end to the midpoint of the beam, while the position of the second crack moved from the midpoint of the beam to the free end of the beam. The position of the first crack gradually moved toward the free end of the beam with increasing cantilever beam frequency. When the crack positions were constant, the natural frequencies of the cracked cantilever beam were inversely proportional to the crack depth and tip mass.

Tables 3 and 4 give the natural frequencies of double-cracked circular and rectangular cantilever beams with tip masses. The positions of the cracks were $\xi_{c1} = 0.3$ and $\xi_{c2} = 0.6$, and the unit of natural frequency was $1/\tau$.

4. Conclusions

The influence of the crack depth, crack position, and tip mass on the dynamic behavior of double-cracked cantilever beams with a moving mass were examined using numerical methods. The cantilever beam was modeled by applying Euler–Bernoulli beam theory. The double-cracked beams were treated as three undamaged segments connected by a rotational elastic spring at the cracked section. The stiffness of the spring depended on the crack depth and geometry of the cracked section. The main results of this study can be summarized as follows.

(1) When the ratio of crack depth was constant, the natural frequencies of the cantilever beam decreased as the moving mass moved to the free end of the cantilever beam.
(2) As the depth of cracks increased, the natural frequencies of a double-cracked cantilever beam with a moving mass decreased. We could determine the position of the cracks in the beam from the sharp change in the slope of the natural frequencies.
(3) When the moving mass was located at the free end of a double-cracked cantilever beam, the frequencies of the cantilever beam were more sensitive to the effect of a tip mass.
(4) When the crack positions were held constant, the natural frequencies of the double-cracked cantilever beam were inversely proportional to the crack depth and tip mass.

Our findings can be used as a basis for analyzing the dynamic behavior of a beam with an arbitrary number of cracks and a moving mass.

REFERENCES

1. Stanisic, M. M., "On a New Theory of the Dynamic Behavior of the Structures Carrying Moving Masses," Ingenieur-Archiv, Vol. 55, No. 3, pp. 176-185, 1985.

2. Lee, H. P., "The Dynamic Response of a Timoshenko Beam Subjected to a Moving Mass," Journal of Sound and Vibration, Vol. 198, No. 2, pp. 249-256, 1996.

3. Yoon, H. I., Jin, J. T. and Son, I. S., "A Study on Dynamic Behavior of Simply Supported Fluid Flow Pipe with Crack and Moving Mass," Proceedings of the 11th International Congress on Sound and Vibration, pp. 2215-2222, 2004.

4. Mahmoud, M. A. and Zaid, C. S. A., "Dynamic Response of a Beam with a Crack Subject to a Moving Mass," Journal of Sound and Vibration, Vol. 256, No. 4, pp. 591-603, 2002.

5. Chondros, T. G., and Dimarogonas, A. D., "Dynamic Sensitivity of Structures to Cracks," Journal of Vibration and Acoustics, Stress, and Reliability in Design, Vol. 111, No. 3, pp. 251-256, 1989.

6. Chondros, T. G. and Dimarogonas, A. D., "Vibration of a Cracked Cantilever Beam," Journal of Vibration and Acoustics, Vol. 120, No. 3, pp. 742-746, 1998.

7. Narkis, Y., "Identification of Crack Location in Vibrating Simply Supported Beams," Journal of Sound and Vibration, Vol. 172, No. 4, pp. 549-558, 1994.

8. Lin, H. P., "Direct and Inverse Methods on Free Vibration Analysis of Simply Supported Beams with a Crack," Engineering Structures, Vol. 26, No. 4, pp. 427-436, 2004.

9. Liu, D., Gurgenci, H. and Veidt, M., "Crack Detection in Hollow Section Structures Through Coupled Response Measurements," Journal of Sound and Vibration, Vol. 261, No. 1, pp. 17-29, 2003.

10. Yoon, H. I., Choi, C. S. and Son, I. S., "Influence of Moving Mass on Dynamic Behavior of Simply Supported Timoshenko Beam with Crack," International Journal of Precision Engineering and Manufacturing, Vol. 7, No. 1, pp. 24-29, 2006.

11. Ruotole, R., Surace, C. and Mares, C., "Theoretical and Experimental Study of the Dynamic Behaviour of a Double-Cracked Beam," Proceedings of the 14th International Model Analysis Conference, pp. 1560-1564, 1996.

12. Sekhar, A., "Vibration Characteristics of a Cracked Rotor with Two Open Cracks," Journal of Sound and Vibration, Vol. 223, No. 4, pp. 497-512, 1999.

13. Ostachowicz, W. and Krawczuk, M., "Analysis of the Effect of Cracks on the Natural Frequencies of a Cantilever Beam," Journal of Sound and Vibration, Vol. 150, No. 2, pp. 191-201, 1991.

14. Shen, M. H. H. and Pierre, C., "Natural Modes of Bernoulli–Euler Beams with Symmetric Cracks," Journal of Sound and Vibration, Vol. 138, No. 1, pp. 115-134, 1990.

15. Christides, S. and Barr, A. D. S., "One-Dimensional Theory of Cracked Bernoulli–Euler Beams," International Journal of Mechanical Sciences, Vol. 26, No. 11, pp. 639-648, 1984.

16. Douka, E., Bamnios, G. and Trochidis, A., "A Method for Determining the Location and Depth of Cracks in Double-Cracked Beams," Applied Acoustics, Vol. 65, No. 10, pp. 997-1008, 2004.

17. Takahashi, I., "Vibration and Stability of a Cracked Shaft Simultaneously Subjected to a Follower Force with an Axial Force," International Journal of Solids and Structures, Vol. 35, No. 23, pp. 3071-3080, 1998.

18. Yoon, H. I. and Son, I. S., "Dynamic Behavior of Cracked Simply Supported Pipe Conveying Fluid with Moving Mass," Journal of Sound and Vibration, Vol. 292, No. 3/5, pp. 941-953, 2006.

19. Meirovitch, L., "Principles and Techniques of Vibrations," Prentice Hall, pp. 400-430, 1997.

20. Inman, D. J., "Engineering Vibration," Prentice-Hall, pp. 329-340, 1994.

21. Kisa, M. and Brandon, J., "The Effects of Closure of Cracks on the Dynamics of a Cracked Cantilever Beam," Journal of Sound and Vibration, Vol. 238, Issue 1, pp. 1-18, 2000.